

Microclimate and species composition shape the contribution of fuel moisture to positive fire-vegetation feedbacks

Supplementary information 1

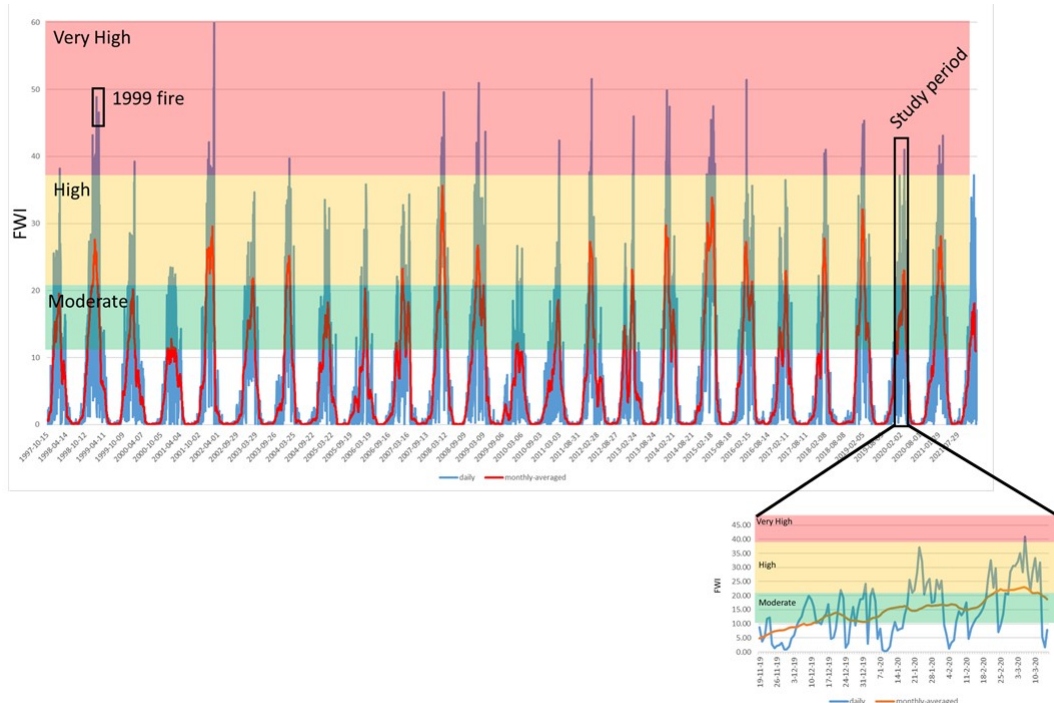


Figure S1. Long-term (1998-2022) (top left) and Nov 19, 2019-Mar 15, 2020 (bottom right) daily (blue line) and monthly averaged (red line) Fire Weather Index calculated using weather forecasts from historical simulations provided by ECMWF ERA5 reanalysis over the study area (European Centre for Medium-Range Weather Forecasts/Copernicus Emergency Management Service). Background colours indicate fire danger classes according to the European Forest Fire Information System (EFFIS; San-Miguel-Ayanz et al., 2012): moderate (11.2 to 21.3; green), high (21.3 to 38; yellow) and very high (38 to 50; red). Black rectangles point to FWI values during the 1999 fire (left box) and during the study period (right box).

Vegetation structure

We recorded species composition to explore its effects on fuel moisture content, and we characterized fuel structure to assesses whether our sites showed the same patterns described by Paritsis et al. (2015) and Tiribelli et al. (2018), where larger sample sizes and study areas were considered. We constructed vertical fuel profiles using the pole intercept method (Paritsis et. al, 2015; Tiribelli et al., 2018). In 30-60 points located in rectangular grids (at least 2 m between points) in each site, we placed a 4 m height pole divided in 16 25-cm segments and recorded presence of fine fuel (leaves or twigs <6 mm) in a 10 cm radius around the pole in each segment, identifying woody species and whether it was live or dead material. We also measured litter bed depth, visually estimated its cover (proportion) in 1 m² quadrats at each point where the pole was placed, and we estimated the canopy cover at 1.5 m height in 30 points by site, using a smartphone and the HabitApp app (Macdonald and Macdonald, 2016). In general, vegetation structure patterns matched those reported by Paritsis et al. (2015) and Tiribelli et al. (2018), but the closed shrubland sites might have lower fuel amount than the average estimated by Tiribelli et al. (2018).

Fuel proportion

Fine fuels were mostly composed of live fuel (leaves and twigs <6 mm diameter), and the live fuel proportion (number of point-segments with fuel over the total number of point-segments) was highest in young forests, followed by mature forests or closed shrublands, and reached its minimum in open shrublands. Considering only dead fuels, there was not a clear pattern of variation between communities. Not distinguishing live and dead fuels, we found the same pattern as in live fuels, given that they were the most abundant (Fig. S2).

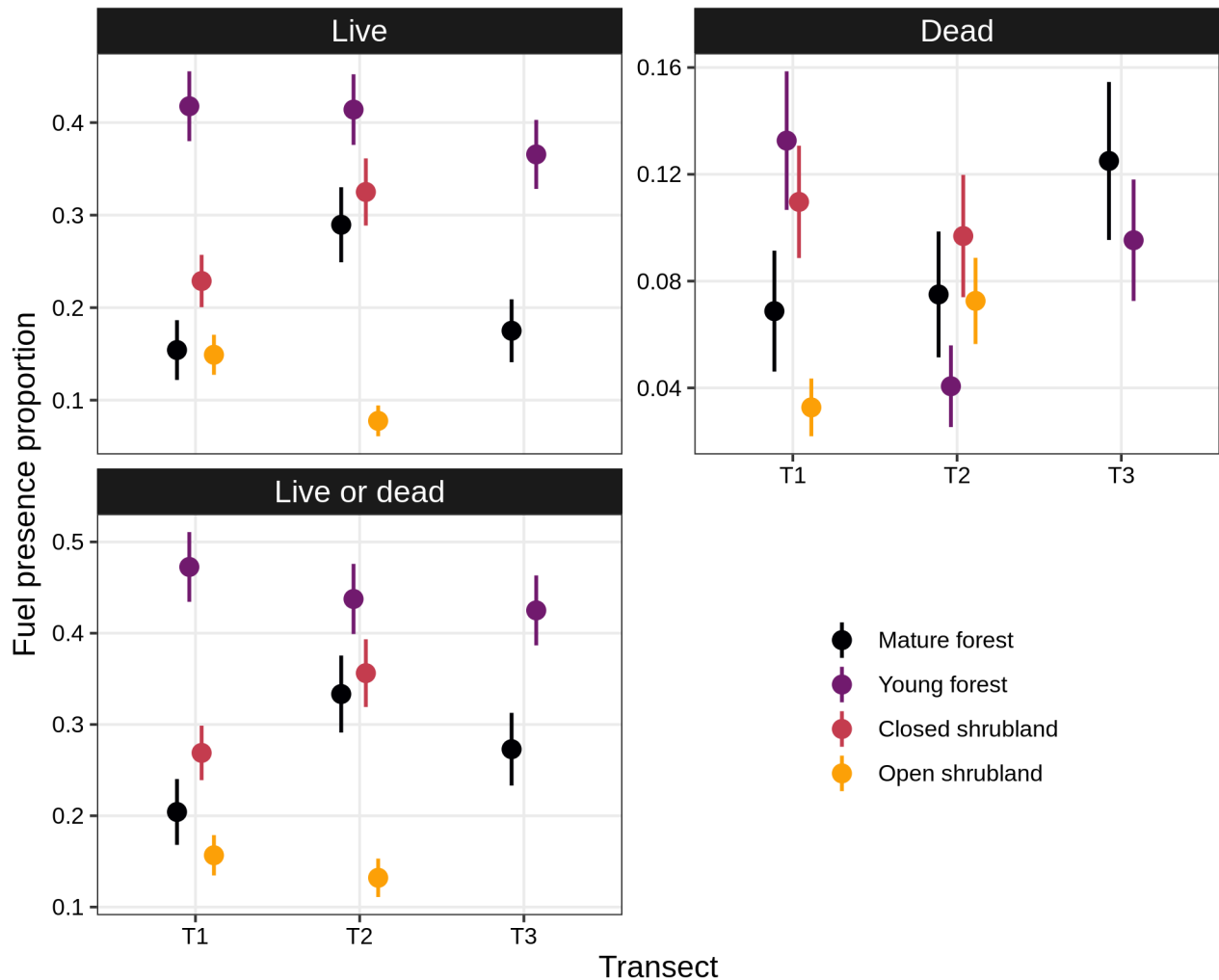


Figure S2. Fuel presence proportion by community and transect. Points show the proportion of pole segments with fuel presence, without distinguishing height and sampling point. As every point had 16 segments (4-m pole, 25 cm by segment), a site with 30 points would have $30 \times 16 = 480$ segments. Bars show ± 2 sd for proportions, computed as suggested by Gelman and Hill (2006; page 17).

Fuel vertical profile

To analyse the vertical continuity of fuels we fitted a binomial generalized additive model where the fuel presence probability varied as a smooth non-linear function of height, which varied between fuel types (live, dead and live or dead), transects and communities. We used cubic regression splines with 11 basis functions, and fitted the model with the mgcv R package (Wood, 2017). The vertical fuel profiles show that young forests show the highest fuel presence probability through all heights, followed by mature forests or closed shrublands. Open shrublands show the lowest fuel presence probability, except at low height, where it is high because of the presence of the grass layer. Closed shrublands show lower fuel presence probability at high height because the shrubs/trees height reached around 3 m, but the fuel continuity is high up to that height (Fig. S3).

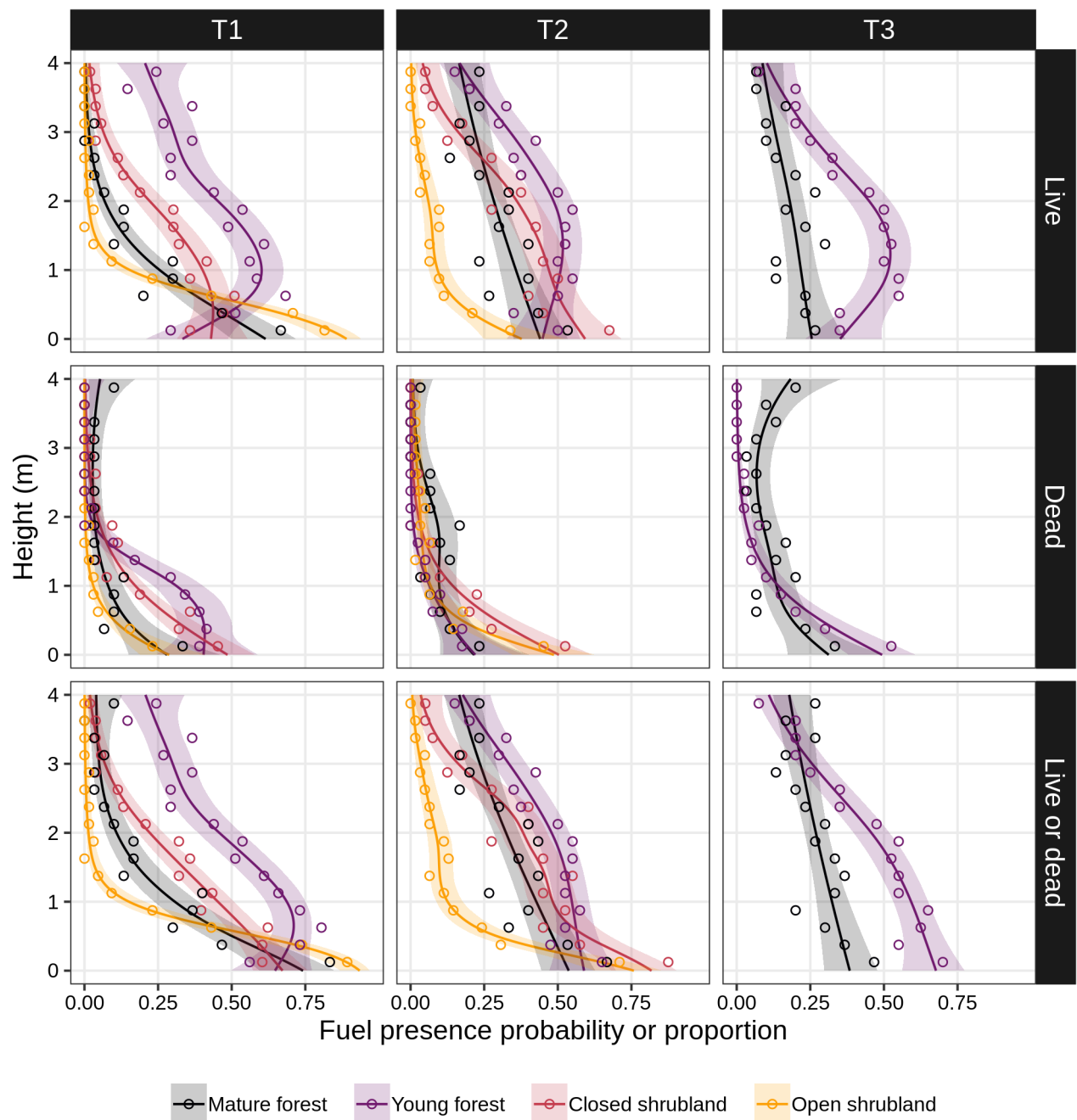


Figure S3. Fuel presence probability (lines) or observed proportion (points) as a function of height, transect and community. Lines show the prediction from the fitted GAM, and the ribbons show the 95 % confidence intervals. The predictor variable is on the y axis to remark that these are vertical fuel profiles. Given our sampling method, the fuel presence probability is interpreted as the probability of finding fine fuel in a 25-cm-height segment centred on a specified height value.

Paritsis et al. (2015) studied alpine *Nothofagus pumilio* forests and nearby shrublands, while Tiribelli et al. (2018) studied *Nothofagus dombeyi* forests and shrublands, as we did. Both studies found similar patterns in general. Tiribelli et al. estimated a higher fine fuel proportion at closed shrublands than in young forests 20 years after the fire, so the opposite difference that we found is probably not a general pattern. Moreover, the closed shrubland at transect 1 had a low fuel proportion compared to Tiribelli and others' predictions.

Notice that as we considered a 10 cm radius to define fuel presence with the pole-intercept method, its reasonable to find values slightly higher than those reported by Tiribelli et al. (2018).

Litter depth and cover

Litter depth in mature forests tended to be lower than in young forests and closed shrublands, but similar or higher than in the open shrublands. Litter cover was lowest in open shrublands, while the differences between the remaining communities were small and variable among transects (Fig. S4).

Canopy cover

Canopy cover showed a large variation among communities. It was highest in mature forests and lowest in open shrublands, and these communities showed low variability. Young forests and closed shrublands showed intermediate values, being higher in young forests, and both communities showed high variability. These patterns were consistent among transects (Fig. S4).

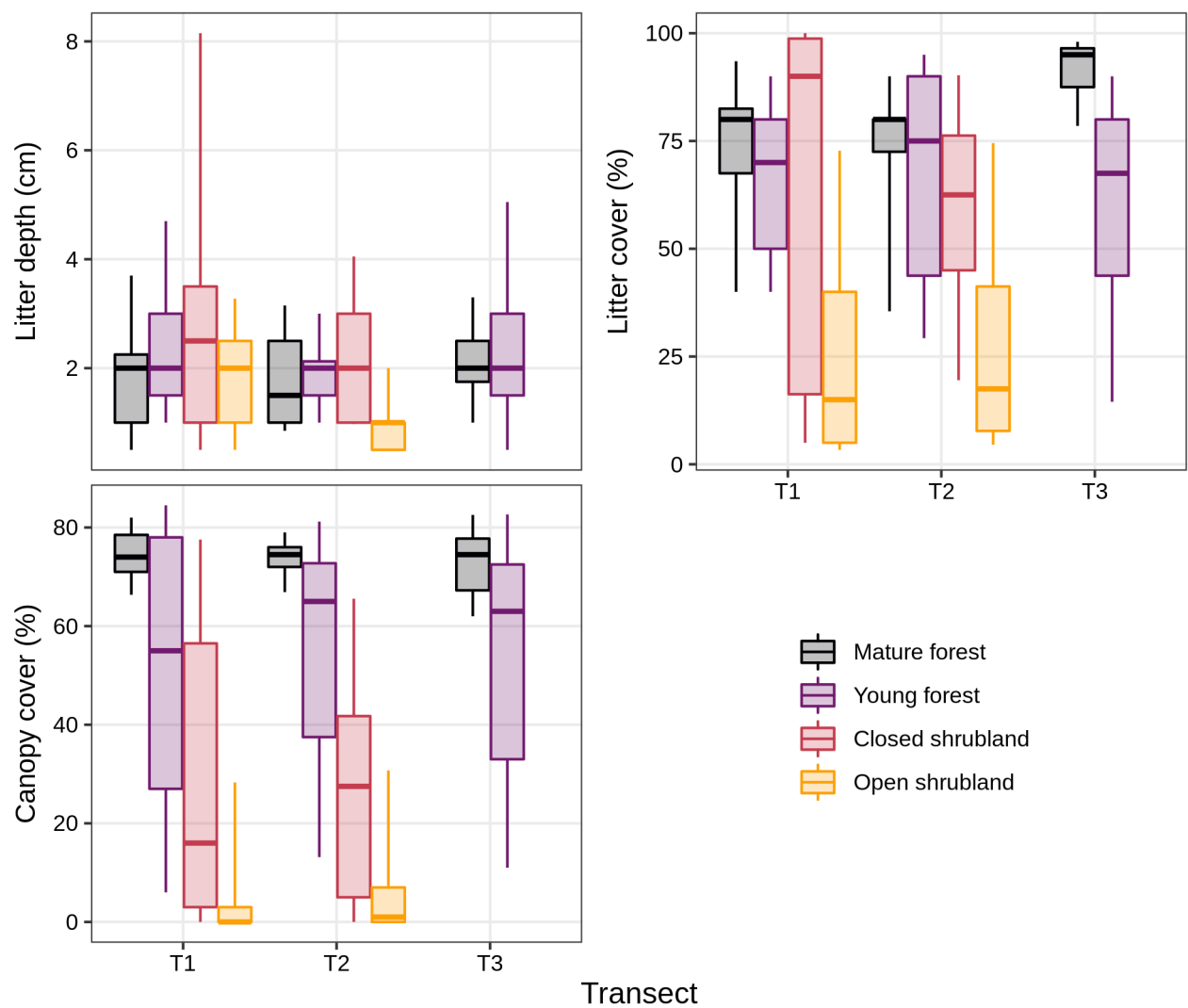


Figure S4. Boxplots for litter depth, litter cover, and canopy cover above 1.5 m height by community and transect (5%, 25%, 50%, 75% and 95% percentiles).

Species composition

Table S1. Relative abundance of species by community and transect considering only live fuel. Species are ordered from most to least abundant, considering all sites together. Relative abundance was derived from the pole intercepts data, describing vegetation up to 4 m height.

Transect ->	T1				T2				T3	
	Mature forest	Young forest	Closed shrubland	Open shrubland	Mature forest	Young forest	Closed shrubland	Open shrubland	Mature forest	Young forest
<i>Nothofagus dombeyi</i>	0.127	0.454	0.000	0.000	0.364	0.791	0.192	0.154	0.093	0.704
Herbaceous	0.127	0.054	0.080	0.626	0.060	0.039	0.129	0.295	0.012	0.074
<i>Schinus patagonicus</i>	0.291	0.086	0.022	0.037	0.212	0.039	0.188	0.269	0.163	0.037
<i>Chusquea culeou</i>	0.253	0.032	0.000	0.000	0.232	0.004	0.000	0.000	0.605	0.144
<i>Mutisia spinosa</i>	0.000	0.146	0.088	0.278	0.000	0.046	0.071	0.000	0.000	0.000
<i>Lomatia hirsuta</i>	0.000	0.143	0.168	0.000	0.000	0.000	0.210	0.000	0.081	0.008
<i>Fabiana imbricata</i>	0.000	0.000	0.195	0.027	0.000	0.000	0.143	0.231	0.000	0.000
<i>Aristotelia chilensis</i>	0.114	0.070	0.000	0.000	0.066	0.039	0.000	0.000	0.000	0.012
<i>Nothofagus antarctica</i>	0.000	0.000	0.190	0.000	0.000	0.000	0.027	0.000	0.000	0.000
<i>Maytenus boaria</i>	0.013	0.000	0.071	0.016	0.000	0.000	0.000	0.013	0.000	0.008
<i>Austrocedrus chilensis</i>	0.076	0.006	0.000	0.000	0.000	0.000	0.000	0.000	0.000	0.000
<i>Berberis microphylla</i>	0.000	0.000	0.027	0.000	0.007	0.014	0.009	0.000	0.012	0.000
<i>Diostea juncea</i>	0.000	0.000	0.044	0.016	0.000	0.000	0.000	0.000	0.000	0.000
<i>Embothrium coccineum</i>	0.000	0.000	0.022	0.000	0.033	0.000	0.000	0.000	0.000	0.000
<i>Discaria chacaye</i>	0.000	0.000	0.044	0.000	0.000	0.004	0.004	0.000	0.000	0.000
<i>Bacaris sp.</i>	0.000	0.000	0.035	0.000	0.000	0.004	0.000	0.000	0.000	0.000
<i>Ribes magellanicum</i>	0.000	0.010	0.000	0.000	0.000	0.011	0.004	0.000	0.000	0.012
<i>Gaultheria mucronata</i>	0.000	0.000	0.000	0.000	0.000	0.011	0.013	0.013	0.000	0.000
<i>Maytenus chubutensis</i>	0.000	0.000	0.000	0.000	0.000	0.000	0.009	0.000	0.023	0.000
<i>Adesmia sp.</i>	0.000	0.000	0.000	0.000	0.000	0.000	0.000	0.026	0.000	0.000
<i>Berberis serratodentata</i>	0.000	0.000	0.000	0.000	0.020	0.000	0.000	0.000	0.000	0.000
<i>Myoschilos oblongum</i>	0.000	0.000	0.013	0.000	0.000	0.000	0.000	0.000	0.000	0.000
<i>Maytenus magellanica</i>	0.000	0.000	0.000	0.000	0.000	0.000	0.000	0.000	0.012	0.000
<i>Rosa rubiginosa</i>	0.000	0.000	0.000	0.000	0.007	0.000	0.000	0.000	0.000	0.000

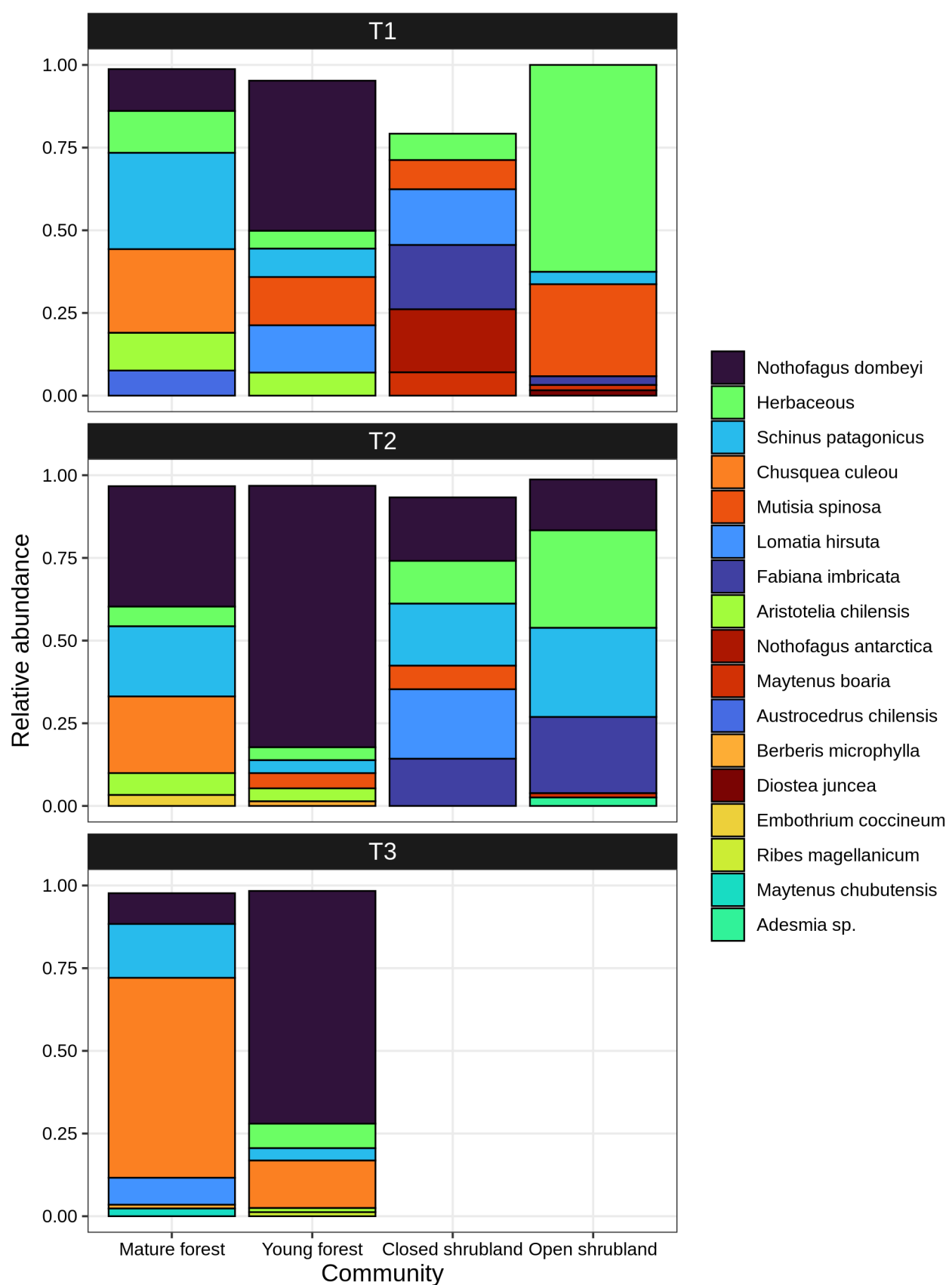


Figure S5. Relative abundance of species by community and transect for live fuel. We only show the six most abundant species in each site for visibility. Relative abundance was derived from the pole intercepts data, describing vegetation up to 4 m height.

Additional figures

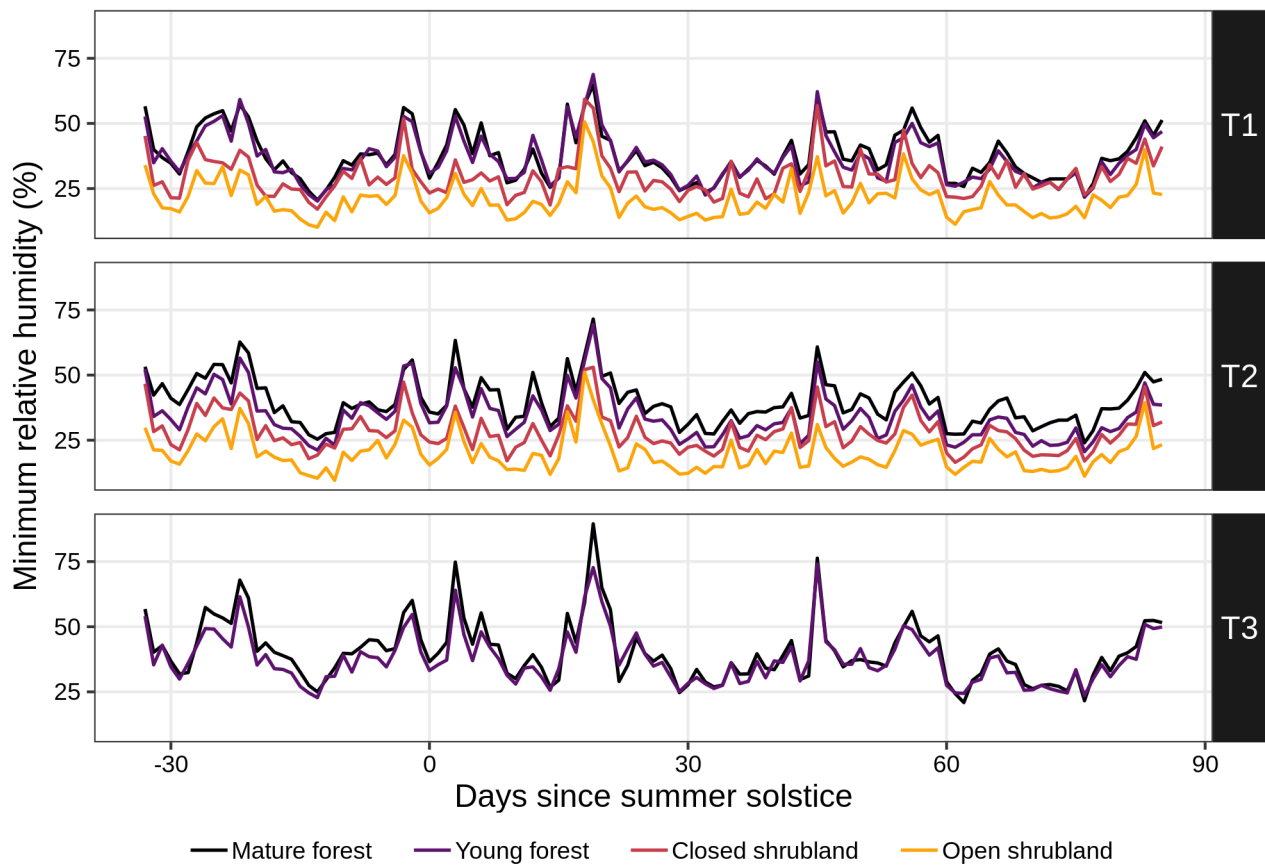


Figure S6. Daily minimum relative humidity (%) throughout the dry season. Day zero is December 21st 2019.

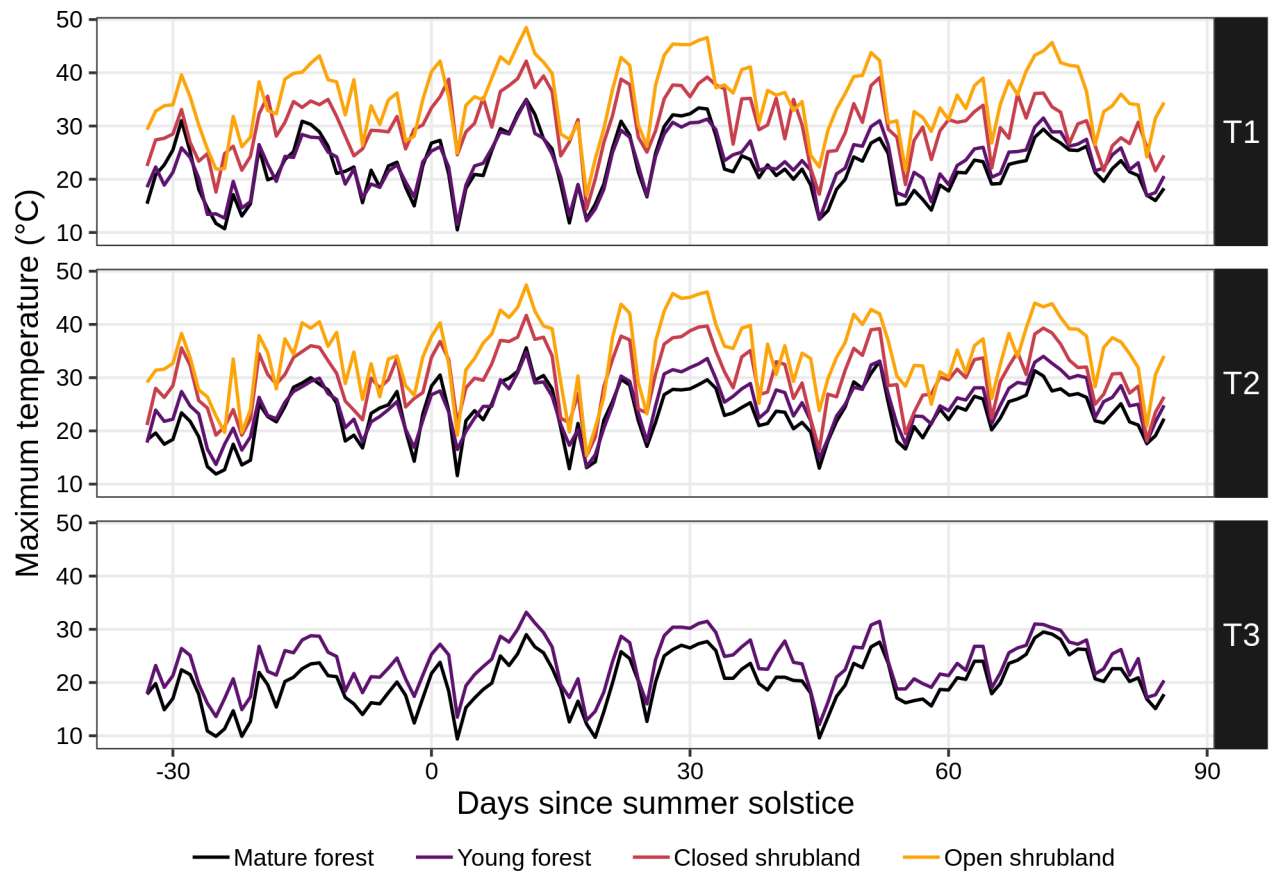


Figure S7. Daily maximum temperature ($^{\circ}\text{C}$) throughout the dry season. Day zero is December 21st 2019.

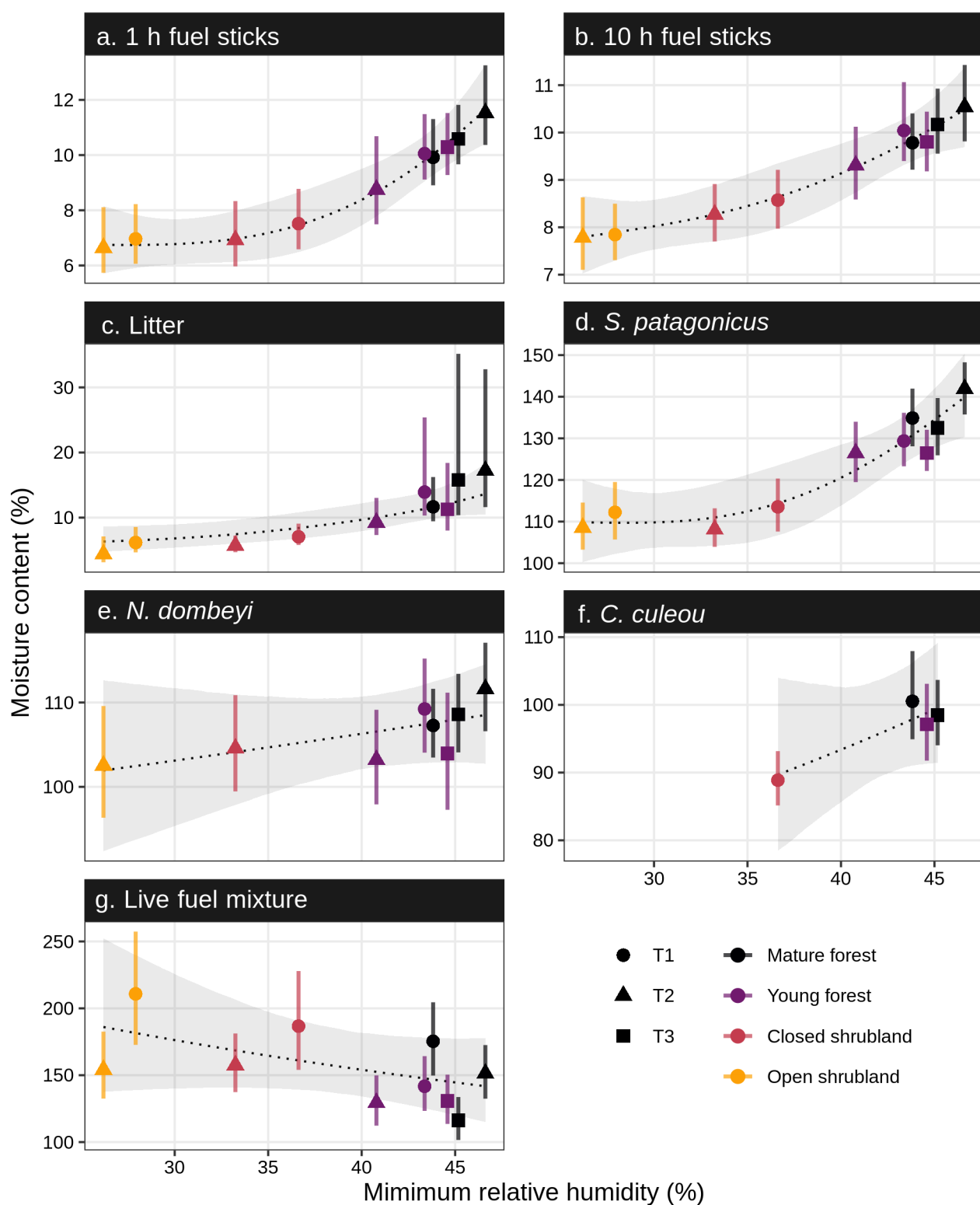


Figure S8. Estimated mean moisture content as a function of the daily minimum relative humidity averaged over the study period by site. Points represent the posterior mean for each site, and bars, the 95% equal-tailed CIs (same values as in Figure 3, right panel). The fitted temperature effect is shown by the dotted line (posterior mean) and the grey ribbon (95% CI). The models followed the same structure and priors as the ones fitted using max VPD, described in the main text and in Supplementary Information 2.

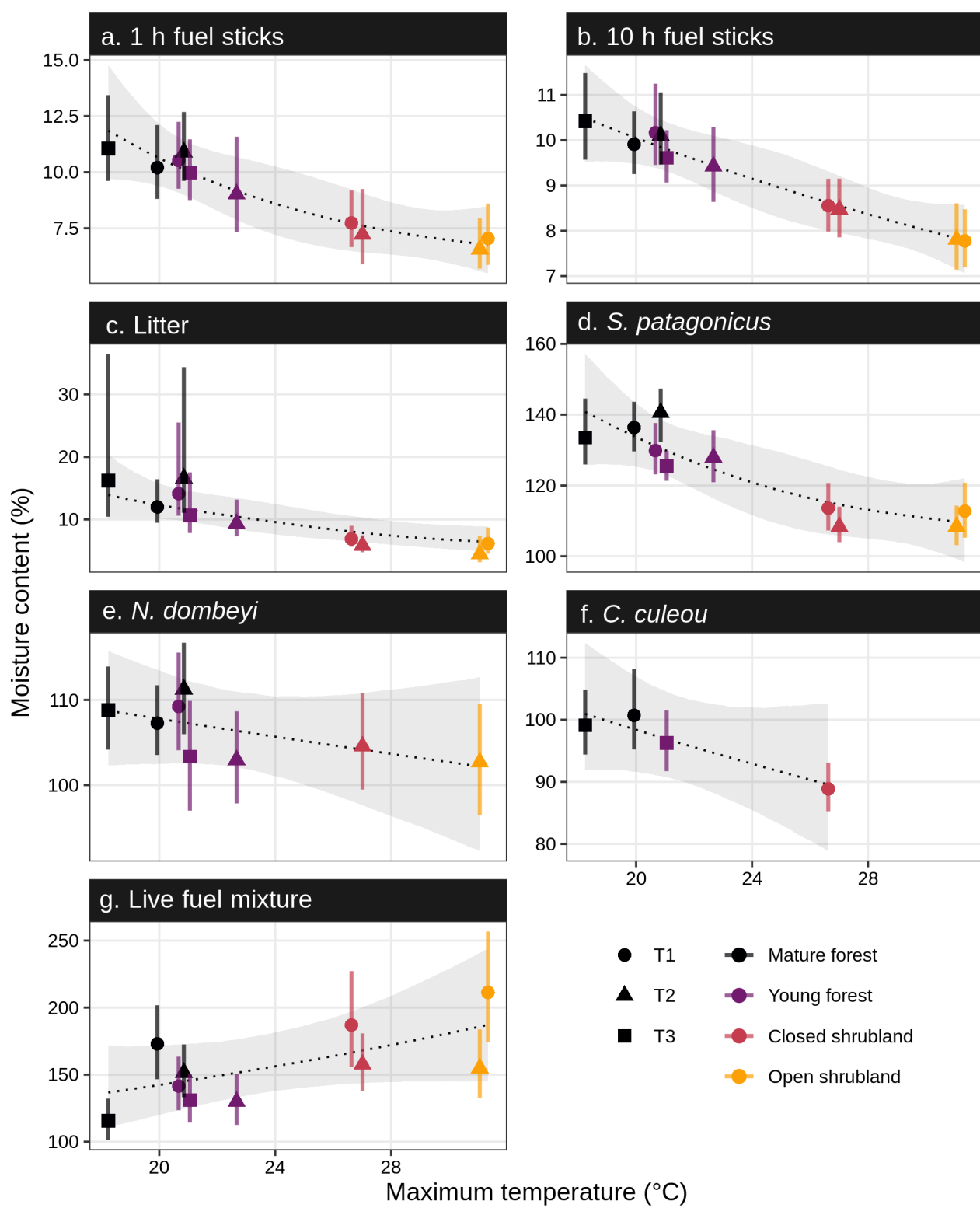


Figure S9. Estimated mean moisture content as a function of the daily maximum temperature averaged over the study period by site. Points represent the posterior mean for each site, and bars, the 95% equal-tailed CIs (same values as in Figure 3, right panel). The fitted temperature effect is shown by the dotted line (posterior mean) and the grey ribbon (95% CI). The models followed the same structure and priors as the ones fitted using max VPD, described in the main text and in Supplementary Information 2.

Figures S10 to S16 (below). Fuel moisture content throughout the dry season by community, transect and fuel type. The line is the mean moisture content estimated by the GLMMs (posterior means), and the darker ribbon is the 95% equal-tailed CI for these means. Points show observed data, and the wider, lighter ribbon shows the 95% Highest Density Interval for the data (where approximately 95% of the points should be). We treated dates as a random effect (categorical variable), but the predictions are connected with lines to improve visibility.

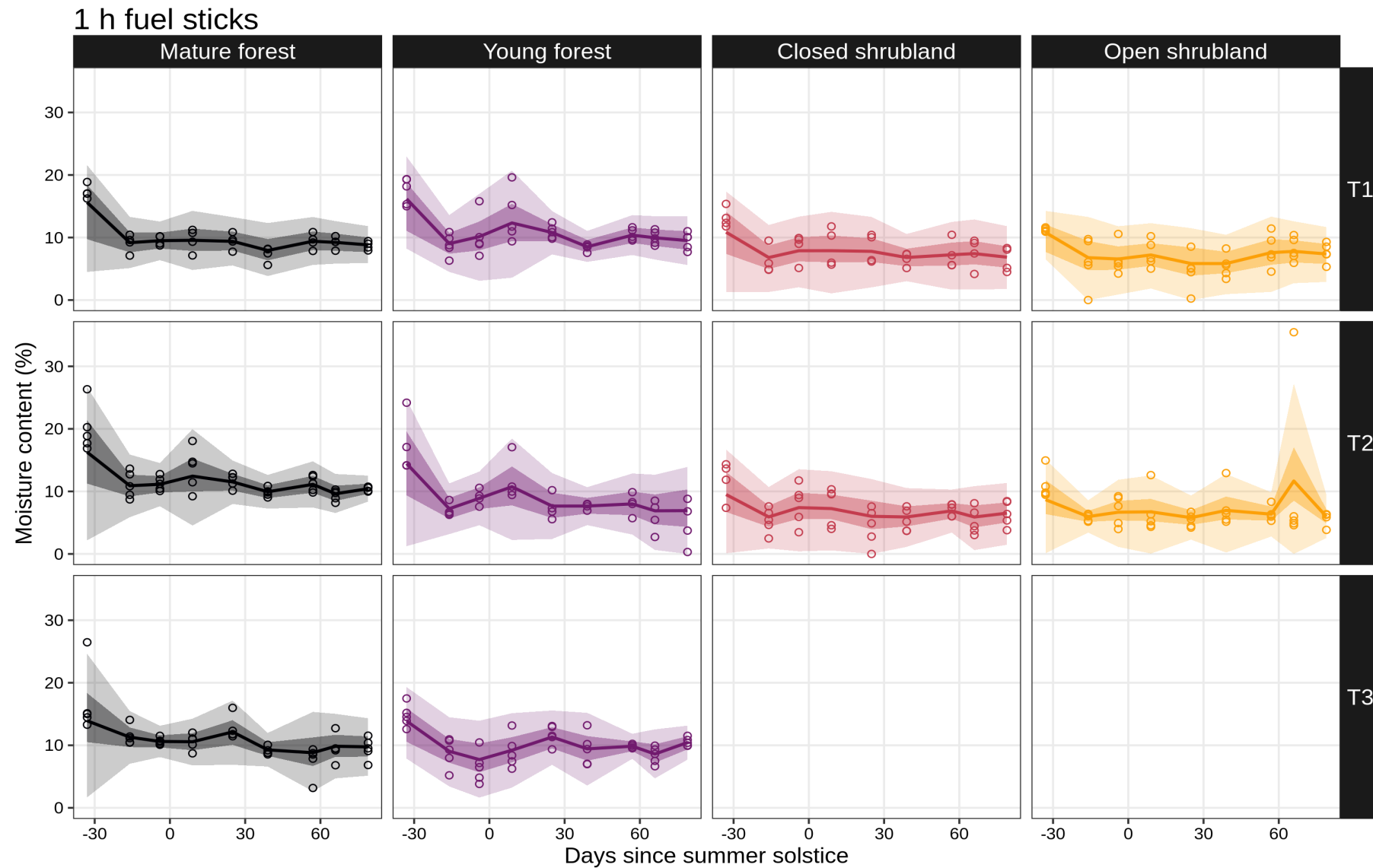


Figure S10.

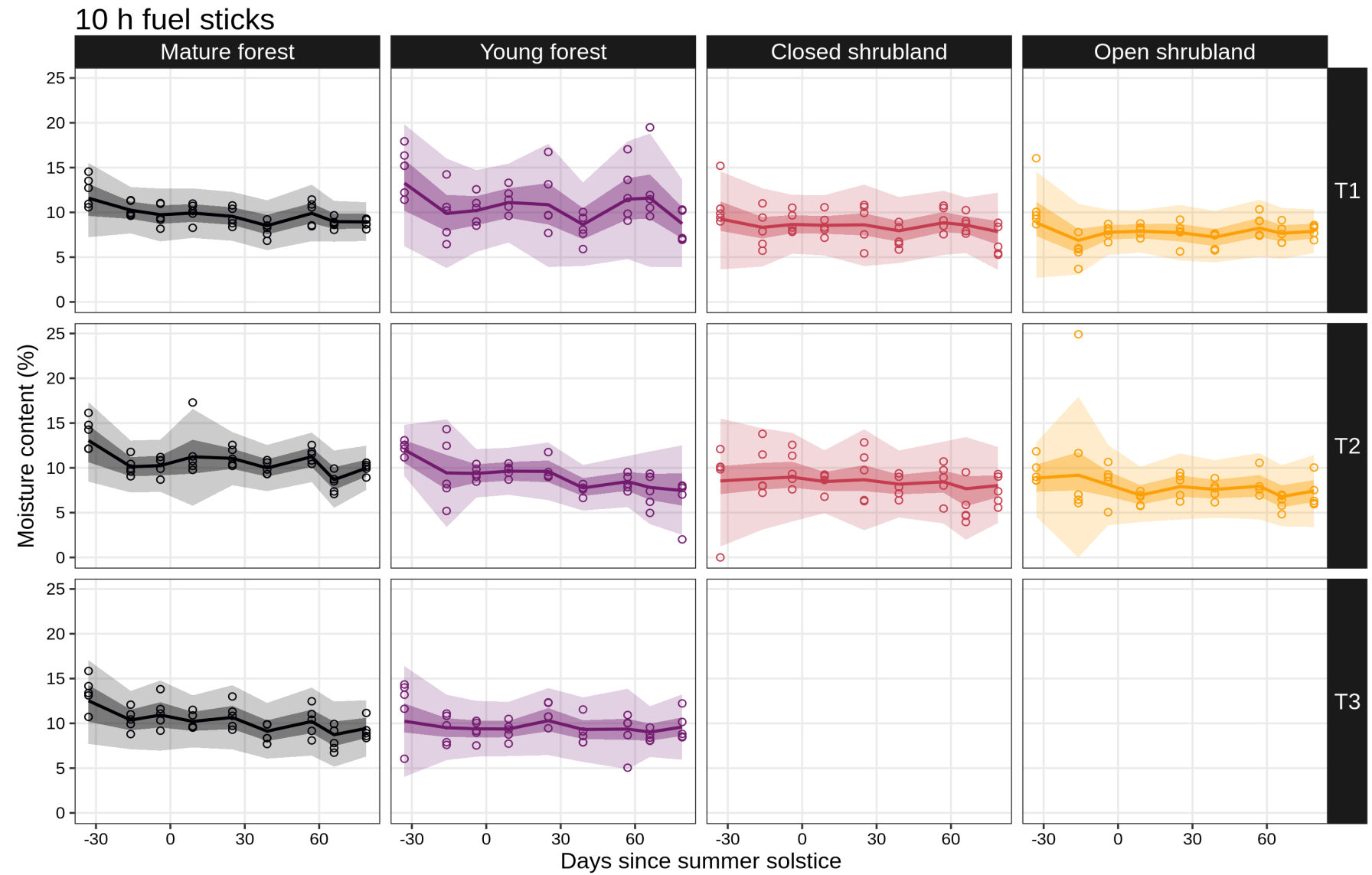


Figure S11.

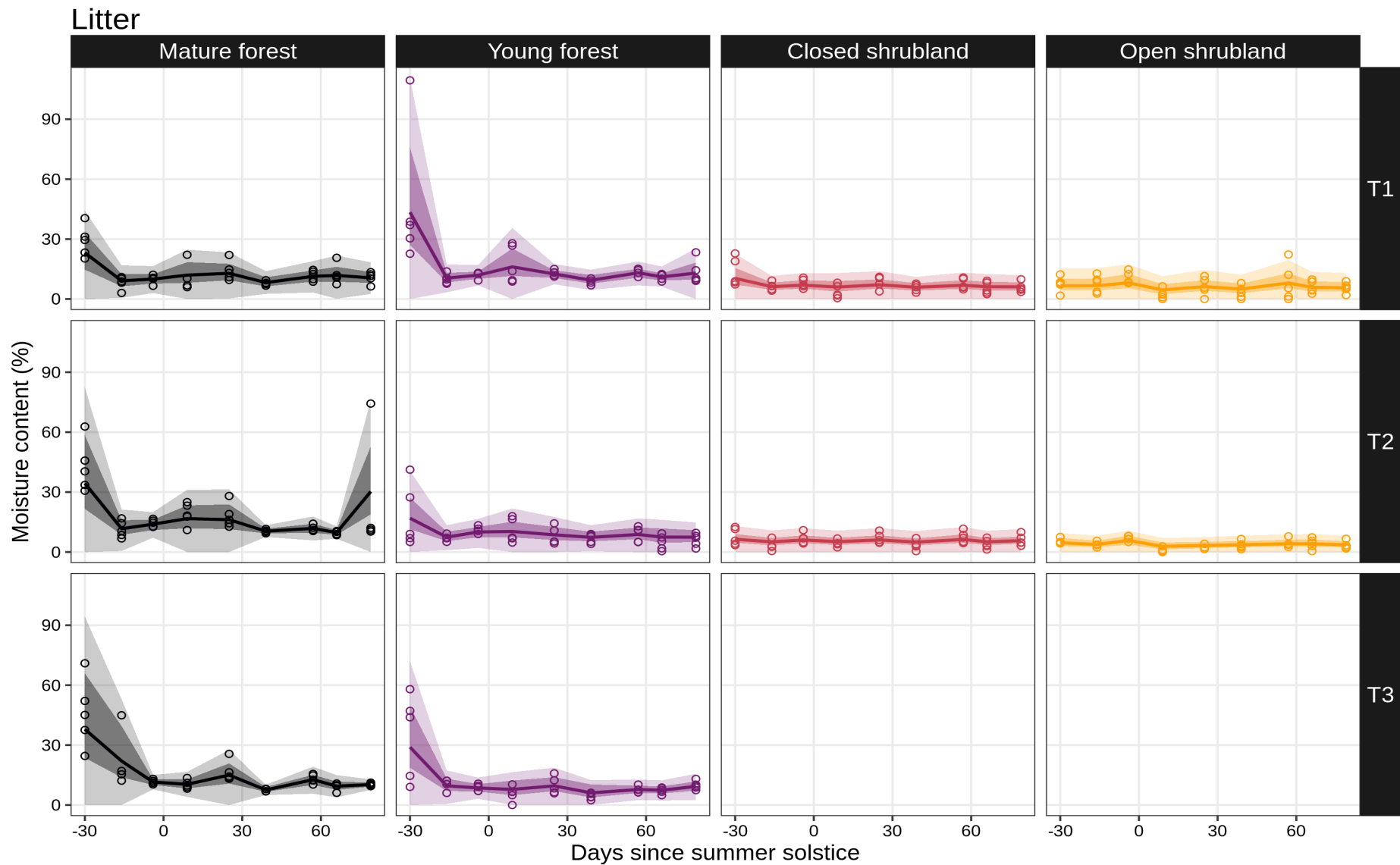


Figure S12.

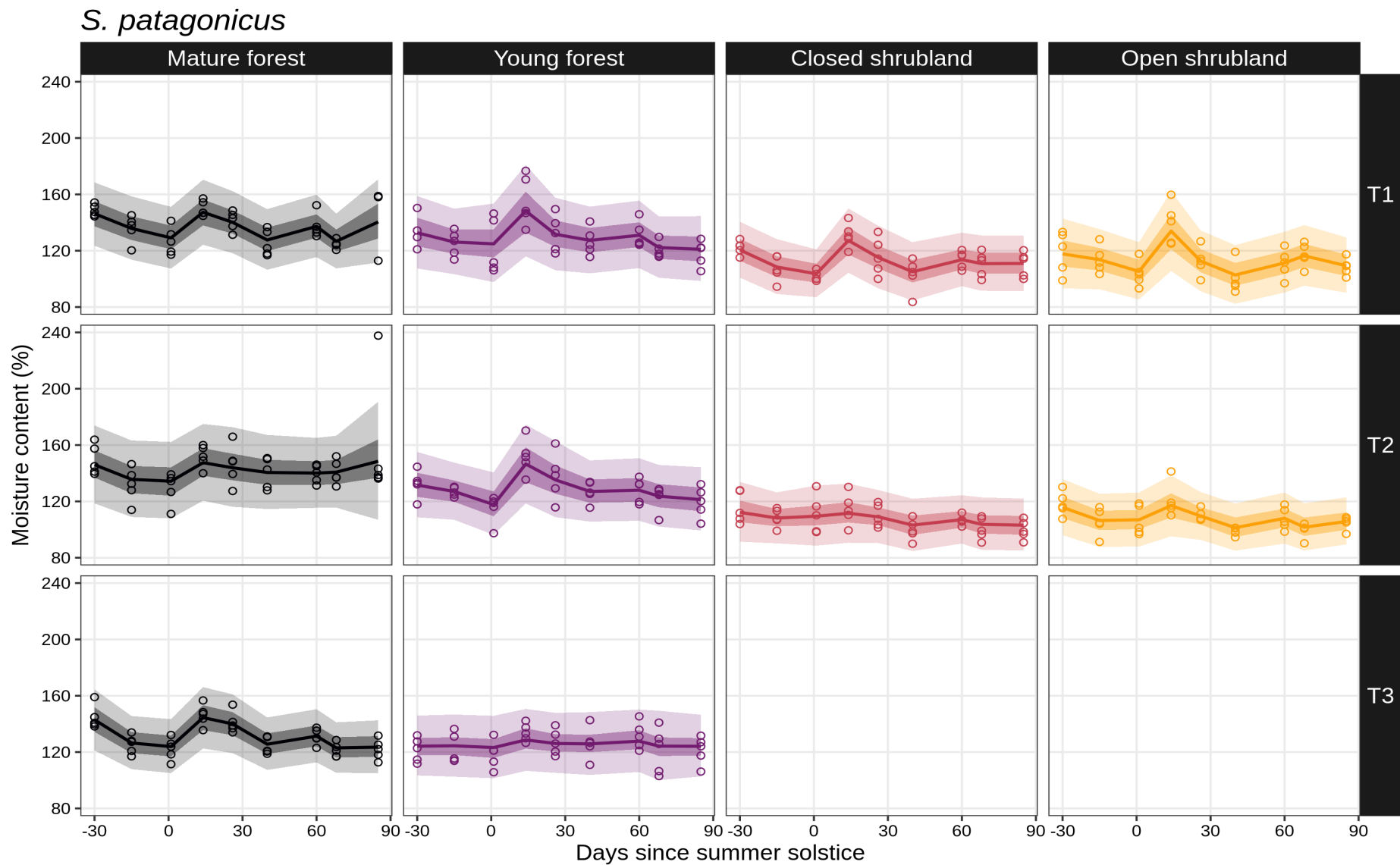


Figure S13.

N. dombeyi

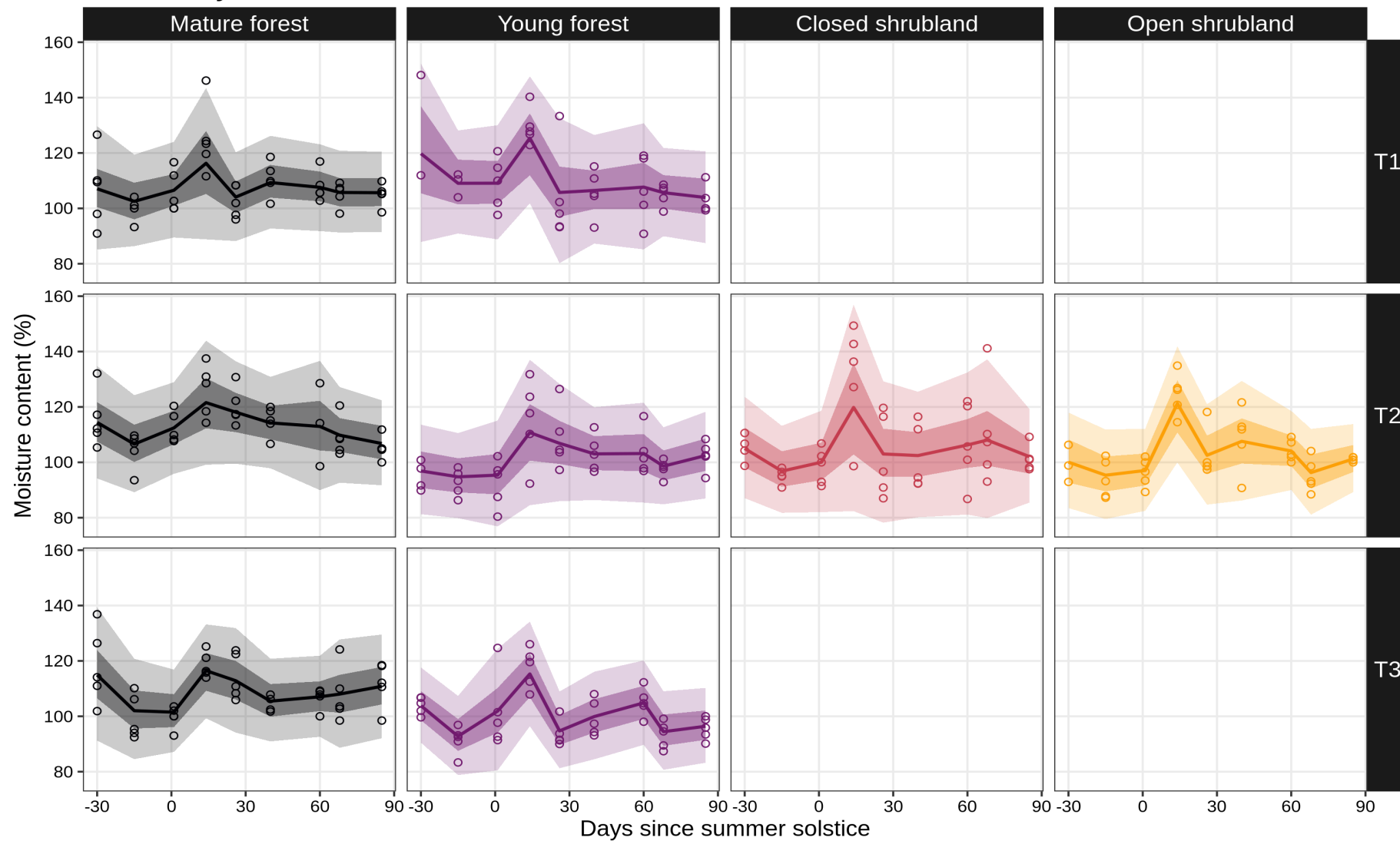


Figure S14.

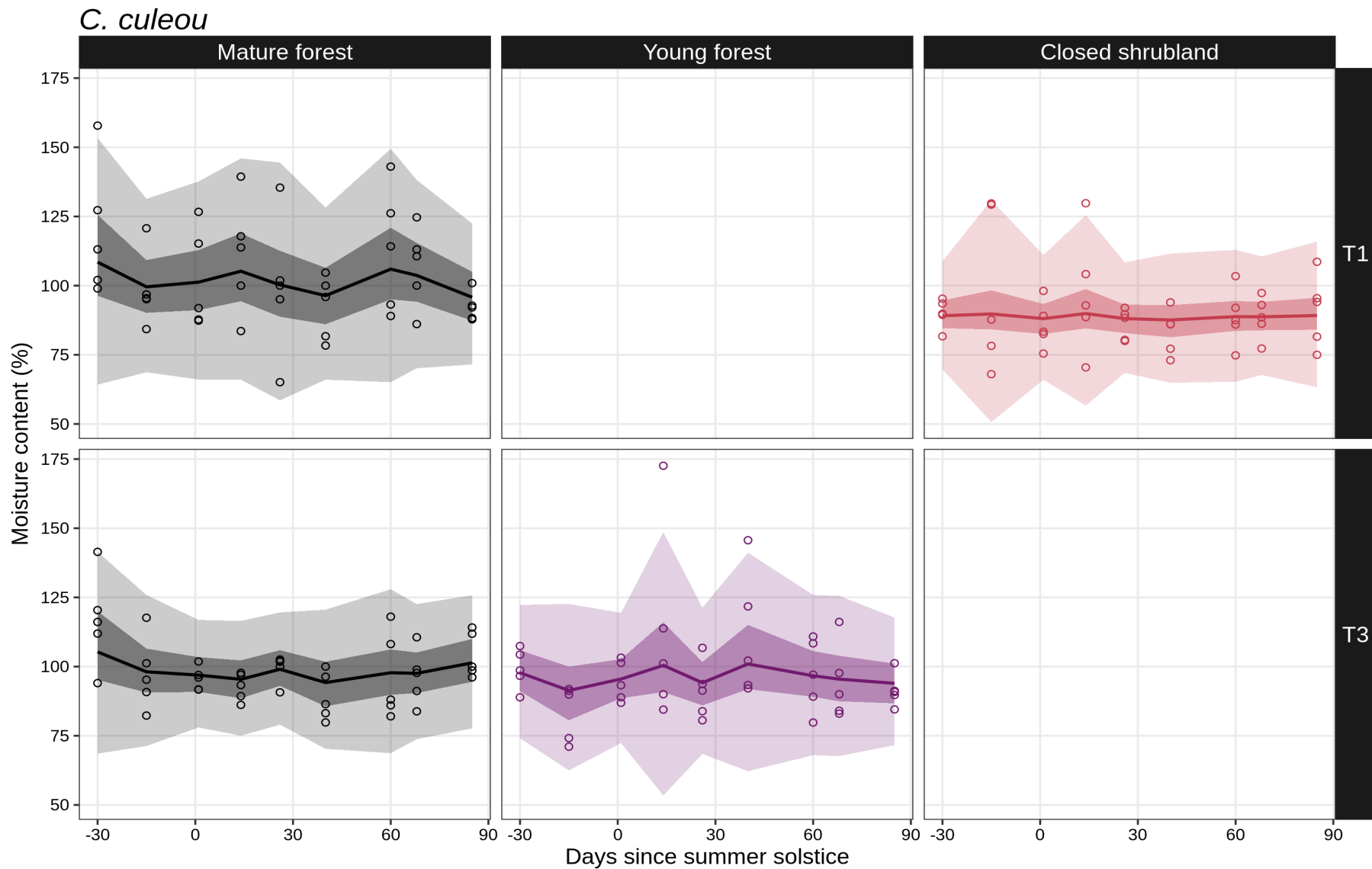


Figure S15.

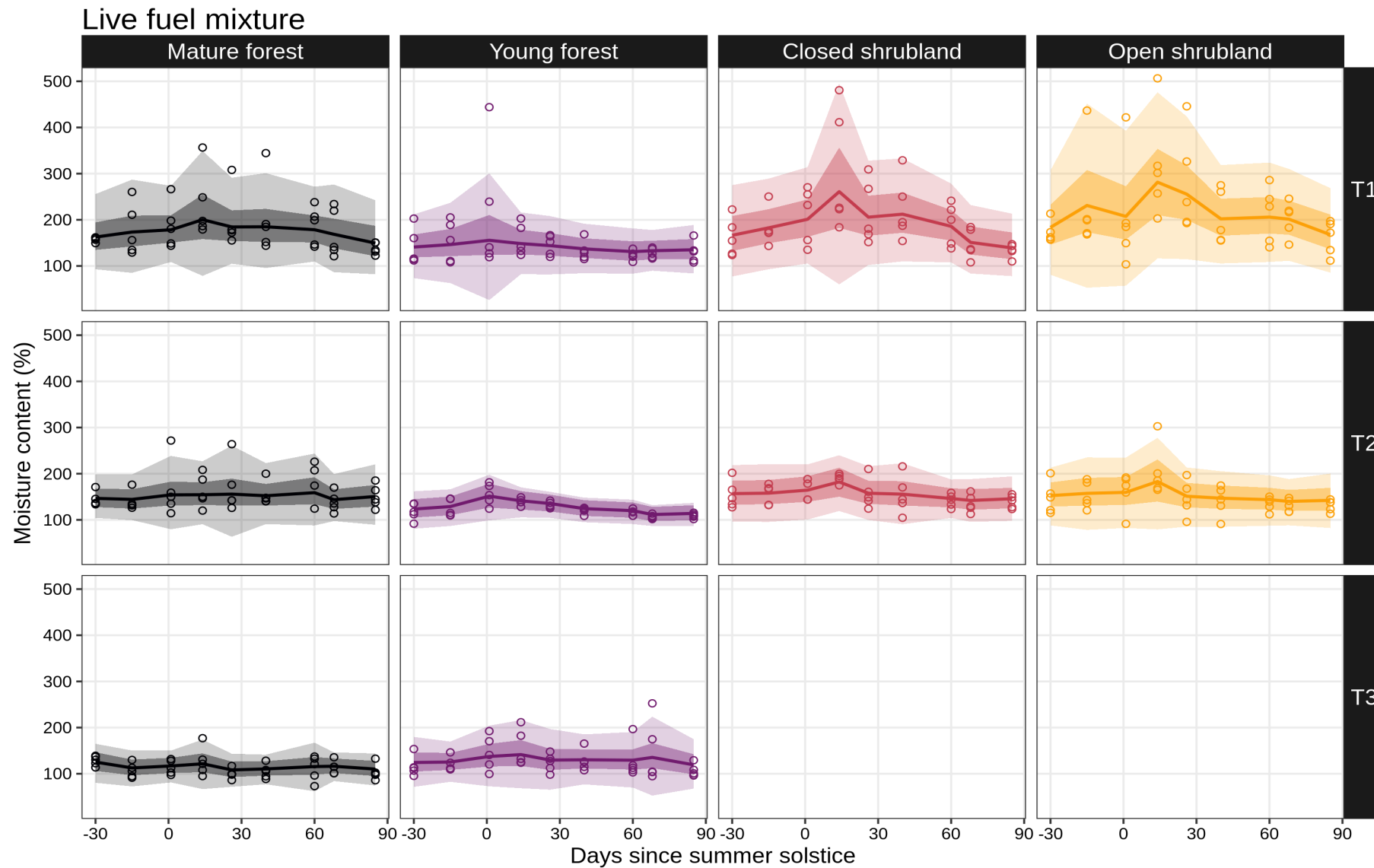


Figure S16.

References

- Gelman, A., Hill, J., 2006. Data analysis using regression and multilevel/hierarchical models. Cambridge university press.
- Macdonald, H., Macdonald, G., 2016. HabitApp. [Mobile Appl]. https://play.google.com/store/apps/details?id=com.scrufster.habitapp&hl=en&utm_source=global_co&utm_medium=prt&utm_content=Mar2515&utm_campaign=PartBadge&pcampaignid=MKT-AC-global-none-all-co-pr-py-PartBadges-Oct1515-1
- Paritsis, J., Veblen, T.T., Holz, A., 2015. Positive fire feedbacks contribute to shifts from *Nothofagus pumilio* forests to fire-prone shrublands in Patagonia. *Journal of Vegetation Science* 26, 89–101.
- San-Miguel-Ayanz, J., Schulte, E., Schmuck, G., Camia, A., Strobl, P., Liberta, G., Giovando, C., Boca, R., Sedano, F., Kempeneers, P., others, 2012. Comprehensive monitoring of wildfires in Europe: the European forest fire information system (EFFIS), in: Approaches to Managing Disaster-Assessing Hazards, Emergencies and Disaster Impacts. IntechOpen.
- Tiribelli, F., Kitzberger, T., Morales, J.M., 2018. Changes in vegetation structure and fuel characteristics along post-fire succession promote alternative stable states and positive fire–vegetation feedbacks. *Journal of Vegetation Science* 29, 147–156.
- Wood, S.N., 2017. Generalized Additive Models: An Introduction with R (2nd edition). Chapman and Hall/CRC.